MECHANIKA TEORETYCZNA
I STOSOWANA
Journal of Theoretical
and Applied Mechanics
1, 31, 1993

INSTABILITY OF THREE DIMENSIONAL BOUNDARY LAYER

EWA SZNITKO

Technical University of Poznań

Design of modern laminar-flow-control aircraft depends on the prediction of the growth of the disturbances in the boundary layer. However, despite large research effort the origins of turbulent flow and the transition process remain one of the most important unsolved problems of aerodynamics. This gives a survey of the experimental and theoretical research on the stability and transition of three dimensional boundary layer. Four types of instability which can occur and lead to transition are analyzed: leading edge contamination, crossflow instability, streamwise instability and centrifugal instability. The e^N method of transition point prediction is discussed.

1. Introduction

Because of the trend in world fuel prices (Fig.1, cf Thomas, 1985) since the early seventies the aircraft drag reduction has become one of the most important tasks for aircraft designers. There are various sources of aircraft drag such as skin friction, left induced drag,separation and wave drag. The greatest contribution is due to a turbulent skin friction drag (about 50% of the total drag, cf Thomas, 1985).

One of the ways of reducing the turbulent skin friction is to delay laminar-turbulent transition on the wing surface as much as possible. This approach is the continuation of the laminar flow control (LFC) programs that were undertaken in England after the second world war. LFC means the maintenance of laminar flow through the use of wall suction (Saric, 1985b; Thompas, 1985). The suction itself cannot suppress any existing turbulence but modifies the curvature of the laminar velocity profile which in turn reduces the amplification of any instability waves in the boundary layer and, in consequence, delays the laminar-turbulent transition.

Fig.2 (Braslow and Fischer, 1985), shows the effect of suction on growth of different types of disturbances. Other physical effects that could be applied to the turbulent skin-drag reduction are the wall cooling and the effect of favourable pressure gradients (natural laminar flow – NLF). A new transition control concept

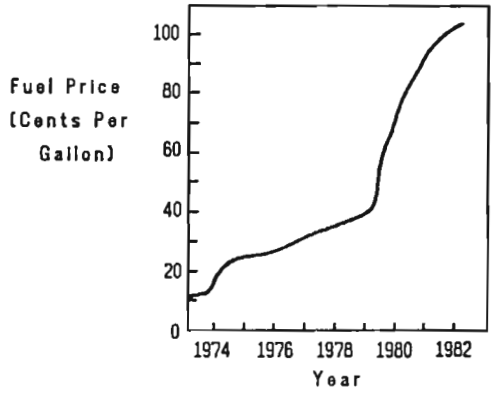

Fig. 1. Trend in world fuel prices

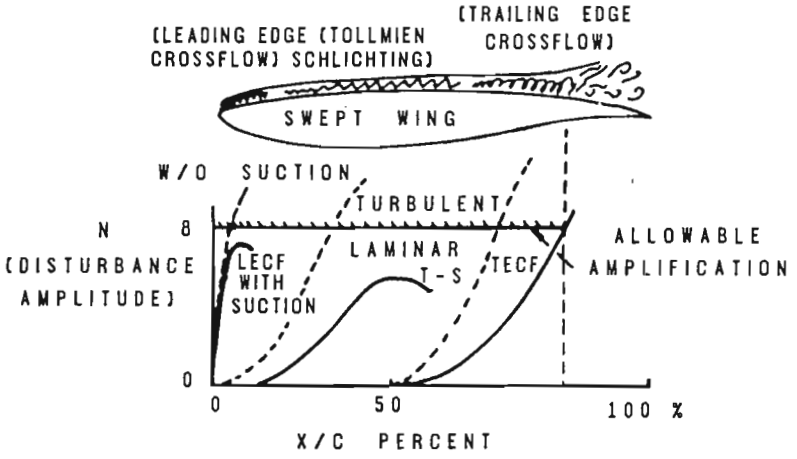

Fig. 2. Scheme of effect of suction on crossflow and Tollmien-Schlichting disturbance growth – amplification rate N versus dimensionless chord x/c for flow with suction an without suction

is to detect any low amplitude pretransitional instability waves in the flow an then to introduce a control disturbance i.e. of equal amplitude and 180 degre out of phase with the original one. Superposition should then remove the prima disturbances from the wall (Thomas, 1985; Braslow and Fischer, 1985; Liepman 1982).

From the aerodynamic point of view, probably the greatest difficulty in i troducing the foregoing ideas is the accurate prediction of where transition w occur. Because our knowledge of transition is not complete, prediction metho to a great extent base on an empirical data. Therefore, the most important ta is to understa d the transition process, which in the future will enable us to pr

dict the point of its location and finally enable us to control the laminar-turbulent transition. The goal of this paper is to describe the generic nature of the laminar-turbulent transition of three-dimensional boundary layer and to show how many unanswered questions we still have.

Shortly, we can describe the transition process in the following way. Disturbances from the freestream enter the boundary layer as steady and unsteady fluctuations. This part of the transition process is called receptivity. The receptivity problem is discussed in Section 2. The instability leading to transition starts with the weak growth of disturbances which can be described by the linear stability theory (the linear stability theory is shortly analyzed in Section 3). When the initially weak disturbances reach a certain amplitude, their development begins to deviate from that predicted by the linear stability theory. Strong three-dimensional (3D) and nonlinear interaction in form of the secondary instability takes place, followed by a rapid growth of disturbances. Then the breakdown of turbulence occurs.

The flow over a swept wing is a typical example of the 3D boundary layer. In this case we have four types of instabilities that lead to transition (Reed and Saric, 1989): leading edge contamination, crossflow instability, streamwise instability and centrifugal instability. The leading edge contamination occurs along the attachment line. This instability is discussed in Section 4. The crossflow instability (Section 5) that occurs within the strong pressure-gradient regions is the dominating type of instability on swept wing. Typically, the upper surface of the airfoil is characterized by an extensive supersonic region preceded by a leading-edge negative pressure peak and followed by a gradual shock-free recompression to subsonic flow with a subsequent rear pressure rise. Consequently, the crossflow instability will dominate before and after of the midchord region (Fig.2, cf Braslow and Fischer, 1985). Steamwise instability (Section 6) is associated with the streamwise component of flow and is similar to processes which take place in 2D flows where Tollmien-Schlichting (T-S) waves are developed. This kind of instability occurs in zero or mild positive pressure gradient region. On a swept wing T-S instability affects midchord region. Centrifugal instability, which can occur on the lower side of the wing, is described in Section 7. A major unanswered question concerns the interaction of different waves, particularly the interaction of crossflow waves with T-S waves. Instability interaction is analyzed in Section 8. In Section 9, e^N transition prediction method is shortly discussed.

2. Receptivity

The boundary layer transition can be interpreted as the consequence of nonlinear response of the laminar boundary layer to forcing free-stream disturbances. The environment in which the boundary layer develops can include different types

of disturbances, such as vorticity, entropy disturbances, surface vibrations etc., or any combination of these. The laminar-turbulent transition process depends very strongly on the nature and spectrum of the free-stream disturbances and on so-called receptivity. By receptivity we mean the way in which particular environment disturbances enter the boundary layer, and the nature of their signature in the flow. If the initial disturbances are small, they will tend to excite free disturbances (normal modes) in the boundary layer. The behavior of these normal modes is usually determined from the linear stability theory (the eigenvalue problem). If the free-stream disturbances are large enough, they can grow by forcing mechanisms leading directly to non-linear levels and then to turbulent flow. Such rapid transition caused by a sufficiently large free-stream turbulence level is called "bypass" by Morkovin (1978).

The receptivity problem, in contrast to normal modes stability calculations, is not a problem with homogeneous boundary conditions. In the receptivity theory the boundary layer is determined by the external forcing disturbances – that is why the response of the boundary layer is the solution of the initial-value problem.

The receptivity problem is described by Morkovin (1978) and Roshotko (1984).

3. Linear stability theory

The historical development of the linear stability theory is described by Mack (1984) and Saric (1985a).

In the linear stability theory, flow parameters are described as a sum of the mean-flow terms (U, W, V, T, Ro, P) and the small unsteady disturbance terms $(u', w', v', \tau', \rho', p')$

$$\begin{aligned} u(x,y,z,t) &= U(x,y,z,t) + u'(x,y,z,t) \\ w(x,y,z,t) &= W(x,y,z,t) + w'(x,y,z,t) \\ v(x,y,z,t) &= V(x,y,z,t) + v'(x,y,z,t) \\ \tau(x,y,z,t) &= T(x,y,z,t) + \tau'(x,y,z,t) \\ \rho(x,y,z,t) &= Ro(x,y,z,t) + \rho'(x,y,z,t) \\ p(x,y,z,t) &= P(x,y,z,t) + p'(x,y,z,t) \end{aligned} \tag{3.1}$$

where u, v, w are velocity components in x, y, z directions respectively; ρ is density; p is pressure; τ is temperature. Assuming that the mean flow is locally parallel (the mean velocity V normal to the surface equals zero and velocity components U, W in streamwise x and apanwise z directions respectively are functions of y), we can describe the disturbances in the following form

$$(u', v', w', p', \rho', \tau')^{\mathrm{T}} = (\bar{u}(y), \bar{v}(y), \bar{w}(y), \bar{p}(y), \bar{\rho}(y), \bar{\tau}(y))^{\mathrm{T}} e^{i(\alpha x + \beta z - \omega t)} \tag{3.2}$$

In Eq (3.2), $\bar{u}(y)$, $\bar{v}(y)$, $\bar{w}(y)$, $\bar{p}(y)$, $\bar{\rho}(y)$, $\bar{\tau}(y)$ represent amplitude functions (complex values); α and β are components of the wave number $\bar{k}$ in x (streamwise) and z (spanwise) direction respectively; ω is frequency. In general case, α, β and ω are complex. If all parameters α, β, ω are real, the wave propagates with constant amplitude in the xz plane. If at least one parameter is complex, the amplitude changes as the wave propagates.

Eqs (3.2) are introduced into the three equations of motion, the equation of continuity and the equation of energy. After linearization we obtain basic equations of the compressible stability theory, which can be written in the following way

$$D\varphi_i(y) = \sum_{j=1}^{8} a_{ij}(y)\varphi_i(y) \qquad i = 1,...,8 \tag{3.3}$$

where

$$\begin{aligned} &D = \frac{d}{dy} \\ &\varphi_1 = \alpha\bar{u} + \beta\bar{w} \quad \varphi_2 = D\varphi_1 \quad \varphi_3 = \bar{v} \quad \varphi_4 = \frac{\bar{p}}{\gamma \mathrm{Ma}_e^2} \\ &\varphi_5 = \bar{\tau} \quad \varphi_6 = D\bar{\tau} \quad \varphi_7 = \alpha\bar{w} - \beta\bar{u} \quad \varphi_8 = D\varphi_7 \end{aligned} \tag{3.4}$$

In Eq (3.4) γ is the ratio of specific heat and Ma_e is the edge Mach number. The boundary conditions are

$$\begin{aligned} &\varphi_1(0) = 0 \quad \varphi_3(0) = 0 \quad \varphi_5(0) = 0 \quad \varphi_7(0) = 0 \\ &\varphi_1(y) = 0 \quad \varphi_3(y) = 0 \quad \varphi_5(y) = 0 \quad \varphi_7(y) = 0 \quad y \to \infty \end{aligned} \tag{3.5}$$

The relations for nonzero elements of the matrix $a_{ij}(y)$ are listed in Appendix 1 (Mack, 1984).

For incompressible flow, from (3.3) we can obtain a single fourth-order equation

$$\left[D^2 - \left(\alpha^2+\beta^2\right)\right]^2 \bar{v} = \mathrm{iRe}\left\{(\alpha U + \beta W - \omega)\left[D^2 - \left(\alpha^2+\beta^2\right)\right] - \left(\alpha D^2 U + \beta D^2 W\right)\right\}\bar{v} \tag{3.6}$$

with the boundary conditions

$$\begin{aligned} &\bar{v}(0) = 0 \quad D\bar{v}(0) = 0 \\ &\bar{v}(y) = 0 \quad D\bar{v}(y) = 0 \quad y \to \infty \end{aligned} \tag{3.7}$$

When $W = 0$ and $\beta = 0$, Eq (3.6) is reduced to the Orr-Sommerfeld equation

$$\left(D^2 - \alpha^2\right)^2 \bar{v} = \mathrm{iRe}\left[(\alpha U - \omega)\left(D^2 - \alpha^2\right) - \alpha D^2 U\right]\bar{v} \tag{3.8}$$

In the above equations, Re is the Reynolds number based on the reference ength and on reference velocity making all quantities dimensionless.

Since the boundary conditions are homogeneous, this is an eigenvalue problem, so that the solution exists only for particular combinations of α, β, ω. The relation of these eigenvalues is called the dispersion relation and can be written in the following form

$$\omega = \Omega(\alpha, \beta) \tag{3.9}$$

The basic task for the linear stability theory is to evaluate the dispersion relation for a given Reynolds number and a basic state $U(y)$, $W(y)$, $P(y)$, $T(y)$, $Ro(y)$. The eigenvalues α, β, ω with the corresponding eigenfunctions $\bar{u}(y)$, $\bar{v}(y)$, $\bar{w}(y)$, $\bar{p}(y)$, $\bar{\rho}(y)$, $\bar{\tau}(y)$ specify the normal mode. The normal modes obtained for 2D boundary layer are called Tollmien-Schlichting waves.

The mathematical form of the wave numbers α, β and frequency ω leads to two theories: the spatial and the temporal one. In the temporal theory frequency is complex ($\omega = \omega_r + i\omega_i$) and α and β are real. In this case the value of wave number $\bar{k}$ is

$$k = \sqrt{\alpha^2 + \beta^2} \tag{3.10}$$

and the angle (so-called wave angle) between the direction of $\bar{k}$ and streamwise direction x is

$$\Psi = \tan^{-1} \frac{\beta}{\alpha} \tag{3.11}$$

The phase velocity has the value

$$c = \frac{\omega_r}{k} \tag{3.12}$$

The imaginary part of frequency ω_i is the amplification rate of the wave

$$\omega_i = \frac{1}{A} \frac{dA}{dt} \tag{3.13}$$

where A represents the value of disturbance amplitude at some particular y (for example y for which amplitude has the maximum value). The disturbances are damped, neutral and unstable for negative, zero and positive values of ω_i, respectively.

In the space theory, ω is real and α and β are complex ($\alpha = \alpha_r + i\alpha_i$, $\beta = \beta_r + i\beta_i$). In this case the wave number vector $\bar{k}$ has the value

$$k = \sqrt{\alpha_r^2 + \beta_r^2} \tag{3.14}$$

The wave angle is defined

$$\Psi = \tan^{-1} \frac{\beta_r}{\alpha_r} \tag{3.15}$$

and the phase velocity is

$$c = \frac{\omega}{k} \tag{3.16}$$

The growth of the waves is

$$-\alpha_i = \frac{1}{A}\frac{dA}{dx} \tag{3.17}$$

The disturbances are damped, neutral and unstable for positive, zero and negative values of α_i, respectively.

The temporal theory is simpler from the computational point of view, because with α, β real and ω complex, there are fewer terms to compute than in the spatial theory. However, the spatial theory corresponds more closely to the usual physical situation. To convert the temporal amplification rate to the spatial one so-called group velocity is used. The group velocity is, in a conservative system, the velocity of propagation of such overall quantities as the energy of the wave packet (every single wave propagates with the phase velocity). By a conservative system we mean the system where energy is not exchanged between the waves and the medium. But instability waves in the boundary layer don't constitute a conservative system so in general case the group velocity is complex (Mack, 1977 and 1984)

$$\bar{C} = \left(\frac{\partial \Omega}{\partial \alpha}, \frac{\partial \Omega}{\partial \beta}\right) \tag{3.18}$$

We can write (Mack, 1984)

$$\frac{d}{dt} = C_r \frac{d}{dx_g} \tag{3.19}$$

where C_r is the magnitude of vector $\bar{C}_r$ (the real part of group velocity vector) and x_g is the coordinate in $\bar{C}_r$ direction. From Eq (3.19) we obtain the relation for spatial amplification rate in the direction parallel to $\bar{C}_r$ (Gaster's relation)

$$-(\alpha_i)_g = \frac{\omega_i}{C_r} \tag{3.20}$$

The results of the linear stability theory are often shown in the form of a neutral curve separating the region of stable disturbances from that of unstable disturbances. Fig.3 shows an example of such a neutral curve obtained for a Blasius flow (constant amplification rate α_i is analyzed). Frequency F (Fig.3) is defined in the following form

$$F = \frac{2\Pi f \nu}{U_e^2} = \frac{\omega}{\mathrm{Re}} \tag{3.21}$$

where f is the physical frequency. From the neutral curve we can see that a single frequency wave traveling in the laminar boundary layer is at first damped, then amplified and finally damped again. The total amplification rate of a single frequency wave (for the spatial theory) is defined as

$$\frac{A}{A_0} = \exp\left(\int_{x_0}^{x} -\alpha_i dx\right) \tag{3.22}$$

where index o refers to the streamwise position where the wave becomes unstable.

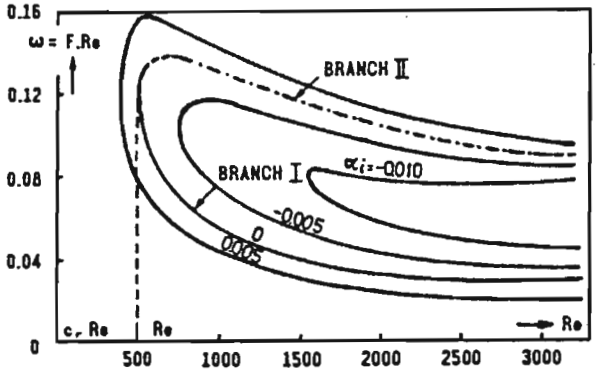

Fig. 3. Stability diagram for the Blasius flow

4. Attachment line contamination

Fig.4a shows the scheme of the flow near the leading edge of the swept wing. The line along which the flow splits over and under the wing (line A–A, Fig.4a) is called the attachment line.

On unswept wings the boundary layer starts at the attachment line and develops towards strong negative pressure gradient, which stabilizes it. Generally, on unswept wings the boundary layer (on smooth surface) remains laminar up to the end of the negative pressure gradient. In the boundary layer on swept wings, the component of the free-stream velocity along the attachment line V_∞ (Fig.4a) gives rise to a spanwise velocity within the boundary layer. In such a boundary layer, disturbances (often coming from the fuselage boundary layer) can propagate spanwise within this layer and, depending on the conditions, instability and transition can occur. Because the boundary layer over the wing originates at the attachment line, transition to turbulence at this line can result in turbulent flow over the whole wing.

The attachment-line boundary layer is characterized by the Reynolds number $\bar{R}$ (Poll, 1981 and 1984)

$$\bar{R} = \frac{V_\infty \eta}{\nu} = \sqrt{\frac{Q_\infty C_0}{\nu} \frac{\sin^2 \vartheta}{U_1}} \tag{4.1}$$

where V_∞ is the spanwise velocity; ν is the kinematic viscosity; ϑ is the sweep of the wing (Fig.4a); C_0 is the chord length measured perpendicularly to the leading edge (Fig.4b); and η is the characteristic length scale

$$\eta = \sqrt{\frac{\nu}{(dU_e/dx)_{x=0}}} \tag{4.2}$$

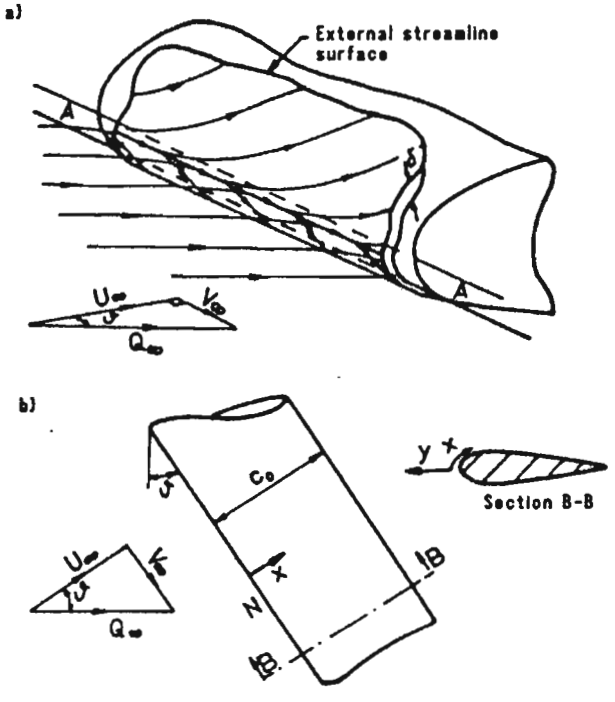

Fig. 4. a) Flow near the leading edge of a swept wing; b) definition and notation

and U_1 is the velocity gradient at the wall (Poll, 1984)

$$U_1 = \left[\frac{d(u_e/Q_\infty)}{d(x/C_0)}\right]_{x=0} \tag{4.3}$$

The transition becomes more likely with the increase of $\bar{R}$. Eq (4.1) shows that the increase of $\bar{R}$ occurs as a result of the increase in the free-stream Reynolds number $(Q_\infty C_0/\nu)$ or the increase in the wing sweep ϑ or in the reducing velocity gradient U_1.

Spanwise turbulent contamination was observed for the first time by Gray (1952) on the aircraft AW52. This phenomenon had been known earlier but the conditions under which it could appear were not documented. The first detailed measurements were made in the 1960's in order to clarify the mechanism which was responsible for the failure of the early laminar-flow swept wing designs. This problem was investigated by Gaster (1967) and later by Poll (1984). The experiments showed that in the presence of large boundary layer tripping devices such as boundary layer fences, 3D roughness elements or 2D trip wires, transition at the attachment line began when $\bar{R}$ reached approximately 250.

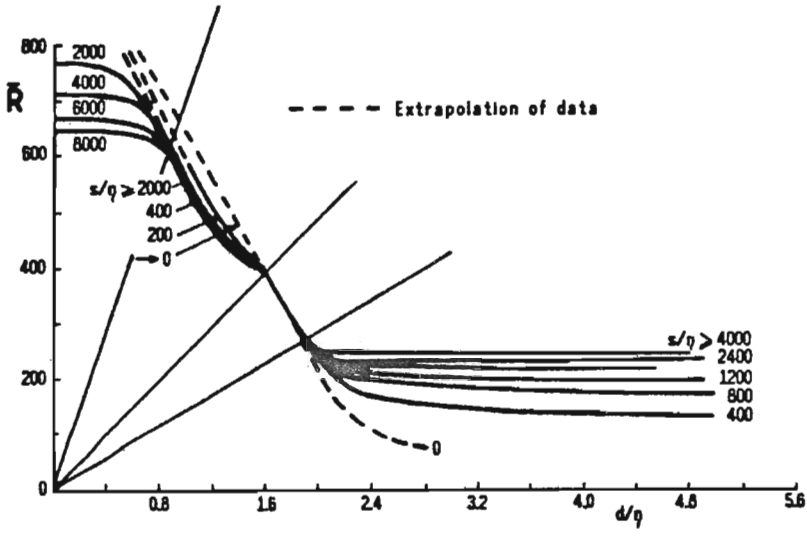

Fig. 5. The variation of $\bar{R}$ with d/η and s/η for the appearence of spots

Poll (1977), (1979) and (1984) provided detailed measurements of boundary layer at the swept attachment line. He investigated the response of the laminar boundary layer of the attachment line to the presence of trip wires of various diameters, arranged so that the wire axis lied in the x direction (Fig.4b). He varied three parameters: the free-stream Reynolds number, the sweep of the wing and the size of disturbances. Fig.5 (Poll, 1984) shows results of these measurements. In this figure the Reynolds number $\bar{R}$ required for the onset of transition is shown versus the nondimensional diameters of trip wires d/η and the nondimensional distance s/η along the attachment line from the point of introduction of disturbance to the onset of transition.

The result presented in Fig.5 indicates that the transition behaviour of the boundary layer of the infinite swept attachment line can be divided into four regimes (Poll, 1984).

The first regime (of high value of $\bar{R}$) is limited by the maximum value of nondimensional disturbance diameter equal approximately to $d/\eta_{max} = 0.8$ (Fig.5). In this regime the transition is the result of the instability of the laminar flow to the small free-stream disturbances. In this case the laminar boundary layer selectively amplifies disturbances of certain frequencies and wave numbers. For swept wing, wave packets are observed near the attachment line for $\bar{R}$ greater than 570. These waves are convected along the leading edge. The disturbance amplitudes increase and eventually the breakdown to turbulence takes place. This process is similar to the one observed in 2D flows (Tollmien-Schlichting waves). Fig.6 (Poll,

1984) illustrates hot-wire measurements of these disturbances.

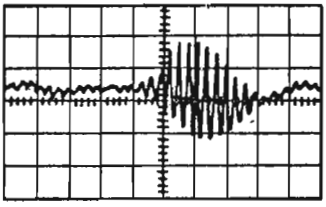

Fig. 6. Hot-wire signals showing the disturbances which precede turbulent spots when $\bar{R}$ exceeds 570

The theoretical aspects of this problem were considered by Hall and Malik (1986) and Hall et al. (1984). They found that the most unstable linear disturbance was the traveling wave of the T–S type.

The point of transition s/η can be predicted by the e^N method. This method, based on the linear stability theory, is analyzed in Section 9. The experimental data indicate that theoretically obtained relations between the transition Reynolds number $\bar{R}$ and the transition distance s/η are correct (Poll, 1984) although the predicted value of transition Reynolds number $\bar{R}$ is about 10% greater than the one observed in the experiments. Despite the differences between theory and experiment, it is clear that the upper limit for maintaining the laminar attachment line is $\bar{R} = 570$. Up to this value the laminar flow is stable to small disturbances. To maintain a laminar attachment line boundary layer for $\bar{R}$ greater than 570, some forms of boundary layer control (suction for example) must be used.

In the second regime the transition occurs for the Reynolds number between 400 and 600 ($0.8 < d/\eta < 1.6$). It is seen from Fig.5 that the distance downstream from the point of introduction of trip wire to the point of occurrence of transition is still large but perturbations which precede the transition are no longer similar to T–S waves. The hot-wire signal of these waves is shown in Fig.7 (Poll, 1984).

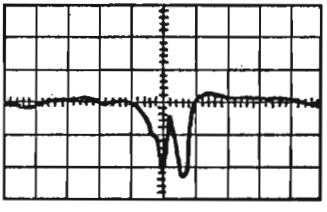

Fig. 7. Hot-wire signals showing the disturbances which precede turbulent spots when $\bar{R} = 495$

For $\bar{R}$ between 250 and 400 ($1.6 < d/\eta < 2.0$) the turbulent spots occur at the trip wire and then propagate along the spanwise direction.

In the last regime, $\bar{R}$ is less than 250 $(d/\eta > 2.0)$. Fig.5 shows that the increase in size of d/η has no effect on the establishment of full turbulence. The turbulence spots still originate at the trip wire but disappear as they convect along the attachment line.

5. Crossflow instability

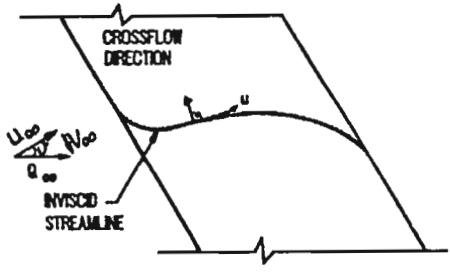

Fig. 8. Scheme of an inviscid streamline over a swept wing

Let us assume that the attachment line boundary layer is laminar and stable to small free-stream disturbances ($\bar{R} < 570$). In the attachment line region both the surface and the flow streamline are highly curved. Along every streamline there is a negative pressure gradient so the flow might be expected to be stable to small disturbances. However, not in this case. The combination of pressure gradient and wing sweep deflects the streamline of inviscid flow in the way presented in Fig.8 (Reed and Saric, 1989). As the result of viscous effects, this deflection is larger in the boundary layer and causes a crossflow. This crossflow velocity component, existing inside the boundary layer, is perpendicular to the inviscid flow velocity vector. The inflection point on the crossflow profile (Fig.9) causes so-called crossflow vortex structure. The reader can find more information concerning the crosflow mechanism in the papers of Saric (1985a) and (1986), Reed and Saric (1989).

The discovery of the crossflow instability is attributed to Gray (1952). Using the sublimation method he discovered closely spaced stationary streaks parallel to the local flow direction in the region near the leading edge of swept wing. These streaks are though to be caused by the action of co-rotating, stationary vortices. Gregory, Stuart and Walker (1955) demonstrated that the same phenomenon existed on rotating disk.

In 1952 Owen and Randall introduced the crossflow Reynolds number defined

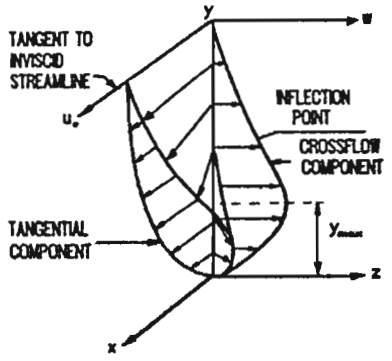

Fig. 9. Scheme of crossflow velocity component

in the following way

$$\mathrm{Re}_{CF} = \frac{W_{CFmax}\delta_{10\%}}{\nu} \tag{5.1}$$

where W_{CFmax} is the maximum crossflow velocity for which $y = y_{max}$ (Fig.9), and $\delta_{10\%}$ is the value of y above y_{max} for which the crossflow velocity is 10% of W_{CFmax}. The crossflow Reynolds number turned out to be very useful in analyzing crossflow fields.

The essential features of a crossflow instability can be studied using the simplest 3D boundary layers of such rotating axisymmetric bodies as disks, cones and spheres. These boundary layers allow for simpler applications of theory and experiments. The exact numerical solution to the Navier-Stokes equation for the laminar mean flow over rotating disk (Karman, 1921), makes this boundary layer particularly profitable to the theoretical stability analysis.

5.1. Experimental work

In the boundary layer of a rotating disk, Gregory, Stuart and Walker (1955), using a china-clay technique, observed $28 \div 31$ stationary co-rotating vortices. These vortices spiralled outward around their logarithmic spiral axes. The angle of the spiral axes with respect to the radius of the disk was $90° + \varepsilon$ (Fig.10) – typically ε is from 11° to 14°. The crossflow vortices appearing in boundary layers of the rotating axisymmetric bodies were recently investigated by many authors (Kohama, 1984a,b, 1985, 1986, 1987a,b,c; Kohama and Kobayashi, 1983a,b; Kobayashi, 1981; Kobayashi and Kohama, 1984; Kobayashi and Izumi, 1983; Kobayashi et al., 1980, 1983, 1987) by a hot wire technique and a smoke visualization

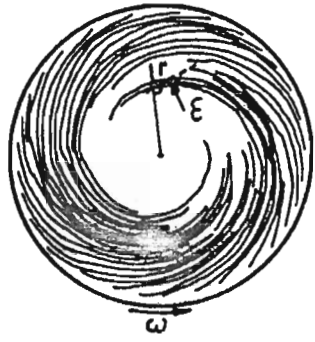

Fig. 10. Scheme of the rotating disk with spiral vortices

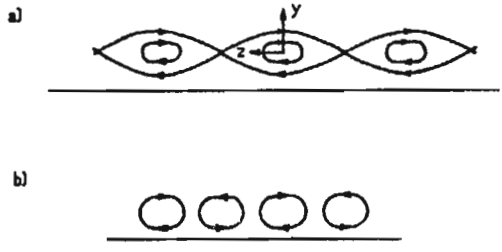

Fig. 11. Schematic of co-rotating a) and counterrotating vortices b)

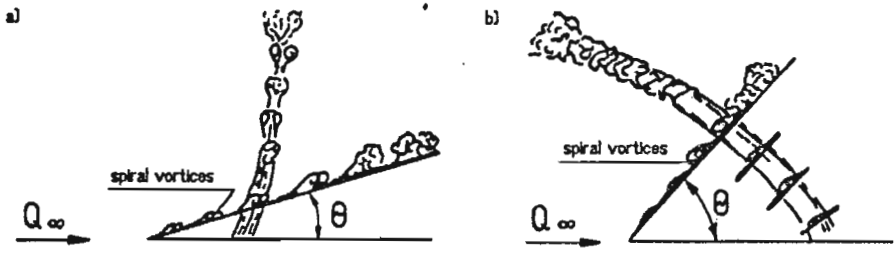

Fig. 12. Schemes of: a) counterrotating vortices; b) co-rotating vortices in the boundary layer of rotating cone

method.

As mentioned above, in the transition region of boundary layer of rotating disk co-rotating vortices appear spirally. In the co-rotating vortex structure all vortices rotate in the same direction and take on the form of so-called "cat's eye" structure (when you look down in the stream direction). This pattern contrasts with the counterrotating structure (Fig.11). It was found that on rotating cone surface there exist two kinds of spiral vortices (Fig.12): co-rotating vortices and counterrotating vortices. In counterrotating structure every vortex winds in the opposite direction to the neighborring vortex. Counterrotating vortices transform to co-rotating vortices when the total angle of the cone Θ and the axial flow velocity exceed certain values. The transformation takes place when the angle Θ is about 30° (Kohama and Kobayashi, 1983).

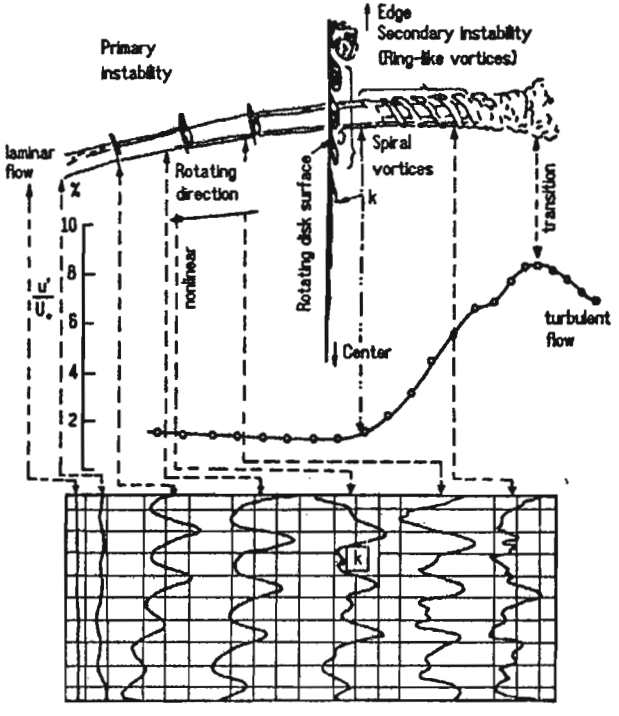

Fig. 13. Scheme of spiral vortice on rotating disk with turbulence intensity distribution and hot wire measurement

Basing on more detailed investigations by close-up camera, we can divide the whole transition region into three stages: primary linear instability, primary nonlinear instability, and secondary instability. All these stages are clearly seen in Fig.13 (Kohama, 1987a), where spiral vortices are sketched. Fig.14a,b,c (Kohama,

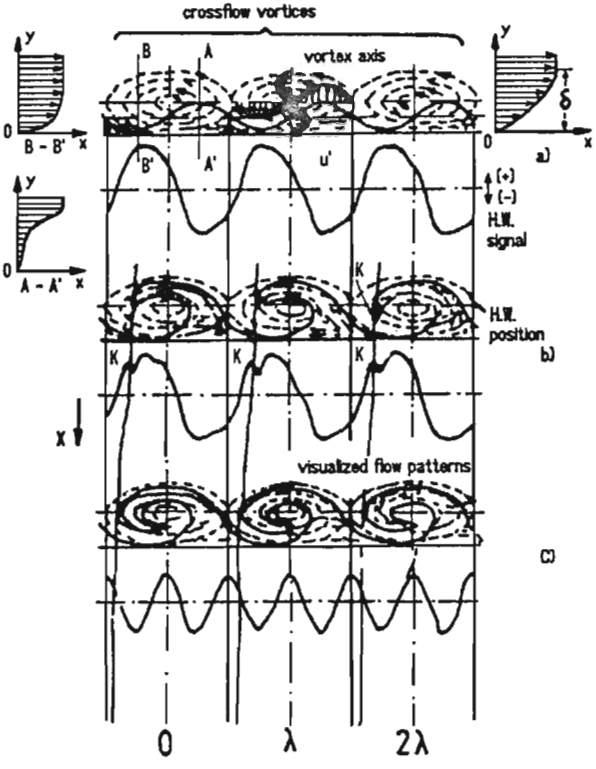

Fig. 14. Scheme of spiral vortices at different sections

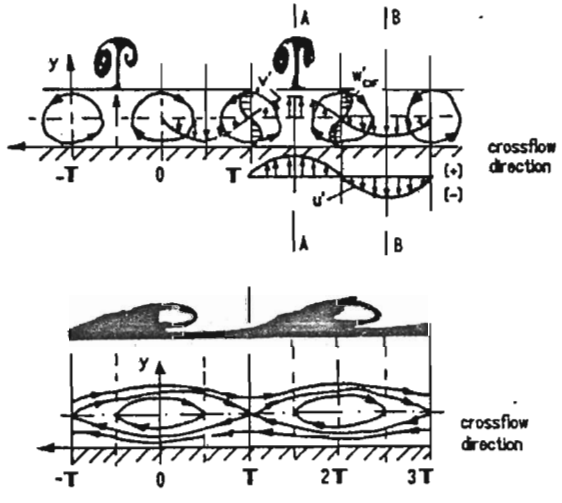

Fig. 15. 3D structure of transition process: a) counterrotating case; b) co-rotating case

1987b) illustrate velocity profiles with the corresponding vortices and hot wire signals for different sections of the spiral vortices – starting at the linear stage and moving downstream. The dark regions correspond to the areas of low velocity (when compared with the velocity of surrounding fluid). The flow pattern changes its structure from the wave shape at the linear stage to the vortex shape at the nonlinear stage.

In the linear part of primary instability we have a sinusoidal hot wire signal of the same frequency as the visualization pattern (in Fig.14. a hot wire measurement of meridional velocity disturbance is shown). At this stage disturbances grow linearly, and the linear stability theory is applicable here.

When the amplitudes of the primary linear waves exceed certain values, a strong nonlinear interaction takes place and higher harmonics are produced. The linear stability theory is no longer applicable. For nonlinear cases (Fig.14b,c), a visualization pattern develops into the curled vortex shape. Here, the primarily sinusoidal hot wire signal is deformed. The kinks in the hot wire signal (indicated by K in Fig.14) correspond to the tips of low speed fluid. As the vortices develop, the intensive mixing of high and low velocity fluid takes place. In section A–A (Fig.15, cf Kohama, 1986) the low velocity fluid from the lower half of the boundary layer is lifted up. At the same time, the high velocity fluid from the upper half of boundary layer (section B–B) is shifted down. The important fact is that as the low velocity fluid is lifted up to the outer edge of boundary layer, a high shear layer with inflectional point appears.

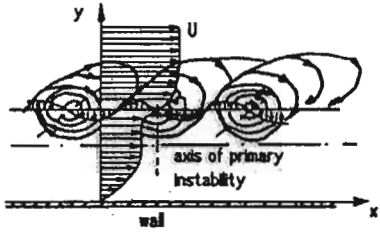

Fig. 16. Scheme of secondary instability

The appearance of inflectional velocity profile gives rise to a new type of instability, called secondary instability. As a result of this, new unsteady disturbances appear on the surface of each primary crossflow vortex (Fig.16, cf Kohama, 1987b). These secondary disturbances, which are initially of the wave type, develop into ring-like traveling vortices. It is interesting to know that traveling vortices of high frequency (about 1kH) travel at the speed of about $U = 0.8U_e$ (Kohama, 1986). Secondary instability depends very strongly on the level of the free-stream turbulence intensity. When the level of turbulence is very high or very low, the

secondary instability is not likely to appear. It is observed only when the intensity of the free-stream is moderate.

In Fig.13 the hot wire signal of secondary instability is shown. The appearance of spike-like signals does not mean that this is a chaotic phenomenon typical for turbulent flow. This signal is the result of the occurrence of two regular disturbances differing in direction and in scale, namely primary and secondary disturbances. It is interesting to notice that the turbulent level at the fully turbulent stage is lower than at the secondary stage.

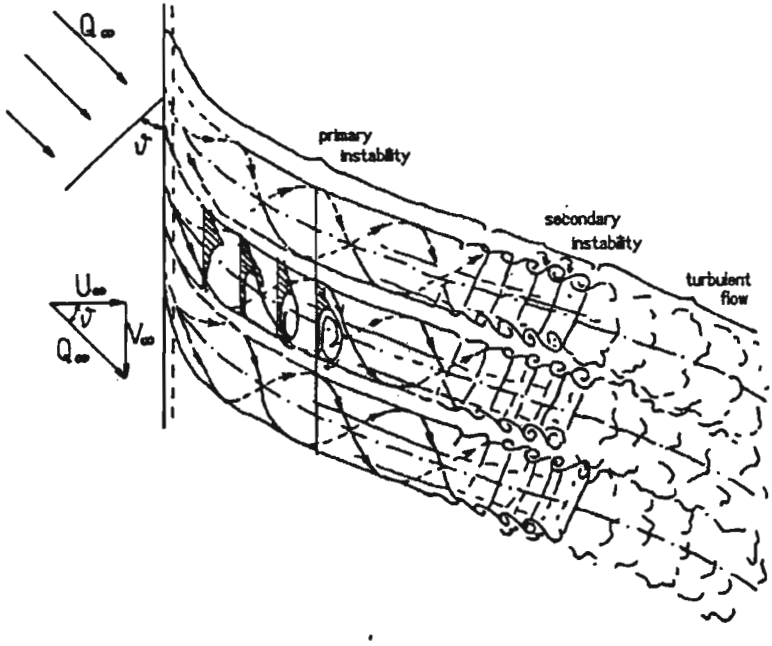

Fig. 17. Scheme of the expected flow field on swept wing

Using all the results concerning the crossflow field, Kohama (1987b) sketched the expected flow on a swept wing in the manner presented in Fig.17. The boundary layer consists of co-rotating spiral vortices. The whole transition region can be divided into primary and secondary instability. The main difference between this flow and that of rotating disk is the absence of the laminar region. The boundary layer is so strongly affected by the negative pressure gradient that the crossflow instability occurs almost immediately downstream of the leading edge. Some information about experimental measurements concerning crossflow vortices in the swept-wing boundary layer can be found by Saric and Yeates (1985).

5.1. Theoretical work

Stuart (Gregory, Stuart and Walker, 1955) derived the 3D linear stability equations (including streamline curvature and boundary layer growth) for parallel incompressible flows. He also determined the transformation for reducing the 3D stability problem to a 2D problem (for the velocity profile in the wave number vector direction). The equations for the linear stability theory of parallel, compressible boundary layer were derived by Lees and Lin (1946) – the work was continued by Lees and Roshotko (1962).

In 1977 Srokowski and Orszag brought out the SALLY code for stability analysis of the parallel 3D incompressible boundary layer on an infinite span swept wing. In spite of using the incompressible stability theory this code was widely used. Then it was superseded by code COSAL (Malik et al., 1982) – compressible version of SALLY. Mack (1979) tested the influence of including compressibility on the stability characteristics (the flow around an infinite span swept wing was considered). He found that the inclusion of compressibility significantly reduced the amplification rate.

In 1981 Padhye and Nayfeh studied nonparallel, incompressible flow over the X-21 wing. They found that the nonparallelism, when regarded, gives more unstable results. Nayfeh (1980) formulated the nonparallel compressible problem (he used multiple scale method) but he didn't present numerical results.

Malik and Poll (1984) found that the inclusion of the streamline and surface curvature in stability calculations had a stabilizing effect on the disturbances (they analyzed incompressible flow around an yawed cylinder). For rotating disk flow again Malik et al. (1981) showed that streamline curvature and Coriolis forces had a stabilizing effect. They calculated temporal eigenvalues which were converted to spatial eigenvalues by using group velocity transformation; Eq (3.20). Then Mack (1985) (following Gaster, 1975) studied stability characteristics of rotating disk spiral vortices. The critical Reynolds number, predicted by Mack, depended very strongly on whether or not the streamline curvature was included.

Singer et al. (1989) studied the nonlinear development of crossflow vortices in an incompressible 3D boundary layer using the weakly nonlinear theory and a direct numerical simulation. Their nonlinear theory is based on the approach of Herbert (1980) and (1983a).

From recent works we know that the linear stability theory used for flow with crossflow component suffers significantly from the discrepancies between theory and experiment. These discrepancies are the result of negligence in calculations of curvature, freestream disturbances and interactions of waves (waves interactions are discussed in Section 8). To avoid all these simplifications, the full Navier-Stokes equations must be solved directly by employing the finite-difference or the spectral methods. In this approach no restrictions with respect to the form of amplitude

of the disturbances are imposed because no linearizations or spatial assumptions concerning the disturbances are necessary. No assumptions concerning the basic flow , such as parallelism, have to be made. The main idea of this approach is to disturb the established basic flow and to analyze the response of the boundary layer.

6. Streamwise instability

Apart from crossflow instability, which is the dominating instability in the 3D boundary layer, there is also the streamwise instability. This kind of instability occurs in zero or mild positive pressure gradient. On a swept wing it occurs in midchord region, which is shown in Fig.2. Streamwise instability is very similar to viscous instability of the 2D boundary layer but with small differences due to the presence of crossflow.

The existence of small, regular oscillations traveling in the 2D laminar boundary layer was first postulated in 1887 by Rayleigh and then by Prandtl (1921). Some years later Tollmien (1935) worked out the theory of boundary layer instability and Schlichting (1933) calculated the total amplification of the most unstable frequencies. In 1947 Schubauer and Skramstad experimentally demonstrated the growth of 2D disturbances leading to laminar-turbulent transition. Physically, the birth of these waves can be related to the concept of receptivity introduced by Morkovin (1978). The instability leading to transition starts with the weak growth of 2D waves called Tollmien-Schlichting waves which can be described by the linear stability theory. When the initially weak disturbances reach a certain amplitude, their development begins to deviate from that predicted by the linear stability theory. This deviation is a result of the quadratic terms neglected in the linear theory which become remarkable and of appearance of the 3D effects. The occurrence of 3D phenomena in an otherwise 2D flow is a necessary prerequisite for transition.

For a moderate Reynolds number ($\mathrm{Re} = U_e\delta_1/\nu$ about 20000 where δ_1 is the displacement thickness), the wavelength $\lambda = 2\pi/\alpha_r$ of these 2D waves lies between 6δ and 18δ (Arnal, 1984). So, the T–S waves are larger when compared with the boundary layer thickness δ. The question is how these harmless 2D waves of large wavelength are related to the violent 3D small-scale and high-frequency motion called turbulence.

Klebanoff et al. in 1962 studied the 3D development of T–S waves under controlled conditions. He performed detailed hot-wire surveys of 3D stages of transition. One of the first observations, using smoke method was made by Brown in 1959 and then by Knapp et al. in 1968. Overall scheme of the transition process made by Knapp is shown in Fig.18.

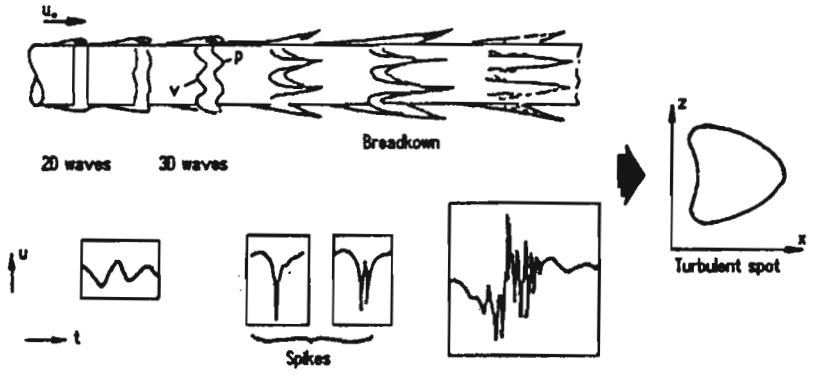

Fig. 18. The transition process in 2D flow-smoke visualizations and typical hot-wire records

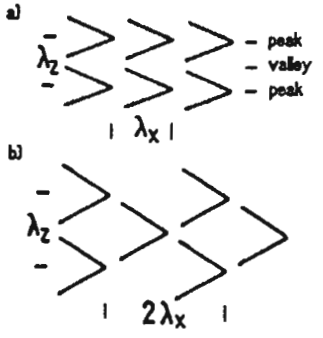

Fig. 19. Peak-valley patterns: a) ordered peak-valley structure, K-type, b) staggered peak-valley structure, C-type or H-type

The appearance of 3D effects was attributed to the spanwise differential amplification of T–S wave. The process leads rapidly to spanwise alternating "peaks" and "valleys" regions of enhanced and reduced wave amplitude (Fig.19, cf Arnal, 1984). The distributions of the streamwise fluctuation intensity at three streamwise positions are shown in Fig.20 (Arnal, 1984).

Regions of maximum and minimum amplitude respectively in this figure correspond to the peaks and valleys. Knapp discovered two clearly distinguished arrangements of the peak and valley structure, which were characterized as ordered structure (Fig.19a) and staggered one (Fig.19b). In ordered structure peaks follow peaks and valleys follow valleys while in staggered structure peaks follow valleys and valleys follow peaks. Recently the experiments showed that a necessary condition for the staggered pattern was the excitation of the subharmonic of the fundamental T–S waves in the boundary layer. Staggered type of 3D transition

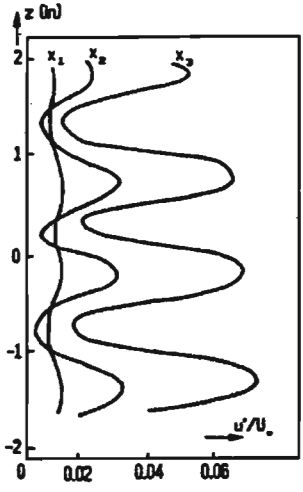

Fig. 20. Spanwise disturbances of u'/U_e at different distances x_1, x_2, x_3 downstream from the source of disturbance

phenomena was investigated by Kachanov el at. (1984), Kozlov et al. (1984), Kozlov and Ramazonov (1984). In fact, two different types of staggered structure have been observed. The subharmonic of the fundamental wave excited in the boundary layer produced either the Craik (1971) resonant wave interaction (C-type structure) or so-called secondary instability of Herbert (H type) (Herbert, 1983b). Saric (1986) pointed out that the important parameter is the maximum value of the primary fluctuation. For amplitudes of the order of 0.3% U_e we have C type structure in which λ_z is larger than λ_x. At amplitudes between 0.3% to 0.6% U_e (H type) λ_x is larger than λ_z. Larger amplitudes of the primary fluctuations lead to the appearance of the ordered structure studied by Klebanoff (K-structure).

In the nonlinear stage of transition the distribution of the mean velocity is distorted – the profiles measured at the peak develop a point of inflection (Fig.21, cf Arnal, 1984). Fig.22 (Arnal, 1984), shows the iso-vorticity contours measured at the peak position (vorticity in this figure is approximated by $(\delta_1/U_e)\partial U/\partial y$). We can observe a considerable increase in spanwise vorticity in the mild part of boundary layer. In Fig.22 T^* represents the period of time of the T–S wave motion. The thin layer of high concentration of vorticity is called high-shear layer. As the flow proceeds downstream, the high-shear layer becomes more and more intense, and finally induces so-called secondary instability (Herbert reserves this term to describe nonlinear process – the Herbert secondary instability). The secondary instability takes the form of a strong negative pulse called "spike" (Fig.18, cf Arnal, 1984). The amplitude of "spike" can reach the value of 30% ÷ 40% U_e. In the later development a second "spike" will appear. Fig.23 (Arnal, 1984) illustrates

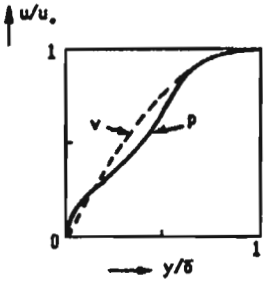

Fig. 21. Mean velocity distribution at peak (P) and valley (V)

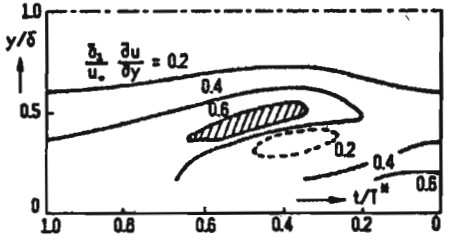

Fig. 22. Contours of approximate spanwise vorticity at peak position, Arnal (1984)

the iso-vorticity contours for one and double "spike" stages, respectively. For each cycle of the primary wave, the number of "spikes" increases and forms bunches of high-frequency fluctuations. That can be interpreted as the division of vortices which are broken down again into smaller vortices. The fluctuations finally take a random character and form turbulent spots. Once created, the turbulent spots are swept along with the mean flow, gradually growing and finally covering the entire surface. More information about secondary instability can be found in Herbert's papers (1984b) and (1988).

In order to explain theoretically the 3D phenomena in the transition region, weakly nonlinear models were primarily developed. The weakly nonlinear theory is in fact a standard perturbation method using expansions about the solution of linear problem (amplitudes of T–S waves are often used as expansion parameters). In this early theoretical work two groups of models were distinguished.

The first group represented nonresonant model. Benney and Lin (1960) studied the interaction between the T–S wave $A(\alpha, 0)$ and the 3D wave $B(\alpha, \beta)$, where α, β are the streamwise and the spanwise wave numbers, respectively. A and B are the amplitudes of the 2D wave and the oblique wave, respectively. This model yields the following amplitude equations

$$\frac{dA}{dt} = A(a_0 + a_1|A|^2 + a_2|B|^2) + a_3 B^2 A^*$$

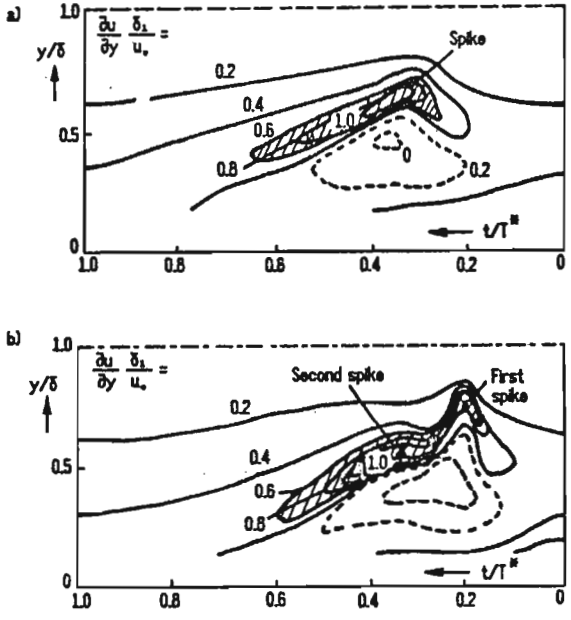

Fig. 23. Contours of approximate spanwise vorticity at peak position, Arnal (1984): a) one spike stage, b) double spike stage

$$\frac{dB}{dt} = B(b_0 + b_1|B|^2 + b_2|A|^2) + b_3 A^2 B^* \tag{6.1}$$

where B^*, A^* are the conjugate amplitudes; a_0 and b_0 are given by the linear stability theory and a_1, a_2, b_1, b_2 are the interaction coefficients.

The second group (resonant) was represented by the Craik resonant triad (Craik, 1971). The triad consisted of the T–S wave $A(\alpha, 0)$ and the two subharmonic oblique waves $B(\alpha/2, \pm\beta)$. The nonlinear interaction analysis led to equations

$$\begin{aligned} \frac{dA}{dt} &= a_0 A + a_1 B^2 \\ \frac{dB}{dt} &= b_0 B + b_1 A B^* \end{aligned} \tag{6.2}$$

The calculations revealed that the nonresonant model (Eqs (6.1)) gives the growth of vortices similar to those reported by Klebanoff. However, this model was unable to estimate the preferred spanwise periodicity. The Craik model (Eqs (6.2)) turned out to be consistent with some experimental observation but was

inoperative in other cases. Both models are discussed more widely by Arnal (1984), Herbert (1988). To avoid all restrictions that usually have to be imposed on the theoretical model, the full Navier-Stokes equations must be solved directly by employing the finite difference or the spectral method (Singer et al., 1986; Orszag and Kells, 1980; Spalart and Yang, 1987; Fasel et al., 1987; Hussaini et al., 1987).

7. Centrifugal instability

Modern supersonic aircraft designs may have regions of concave curvature on the lower side of the wing. It is a well known fact that in the boundary layer over a concave surface a strong centrifugal instability takes place. This type of instability is manifested by the presence of counterrotating vortices, the axes of which are parallel to the principal flow direction (Fig.24a).

Görtler (1954) was the first who studied the counterrotating vortices on the concave surface and this vortex structure beared his name. Later, Wortmann (1969) studied the development of centrifugal instability in a water tunnel with curved walls. He described the transition process on concave surface in the following manner.

The first step in the transition process is characterized by the classic Görtler vortices pattern shown in Fig.24a. We can see a strong spanwise deformation of the mean velocity profile. Then the steady second-order instability destroys the symmetry of the vortices (Fig.24b). The onset of the second-order instability depends on the Reynolds number on one hand and on the intensity of the primary vortices on the other hand. Further downstream the vortices show a characteristic oscillating motion which becomes turbulent a few wavelengths downstream. Wortmann found that these 3D oscillations were not a result of the second but of the third-order instability.

In his theoretical work Görtler assumed that 3D disturbances (superposed on the mean flow) could be described in the following form

$$\begin{aligned} (u', v', p')^{\mathsf{T}} &= (f, \varphi, \pi)^{\mathsf{T}} \cos(\tilde{\alpha} z) F \\ w' &= h \sin(\tilde{\alpha} z) F \end{aligned} \tag{7.1}$$

where in temporal theory $F = \exp(\omega t)$ and in spatial theory $F = \exp(\tilde{\beta} x)$; $\tilde{\alpha}$ was the spanwise wave number; $\tilde{\beta}$ was the streamwise wave number; f, φ, h, π were amplitudes of disturbances u', v', w', p', respectively. Görtler introduced the above relations to the equation of continuity and to the linearized equations of motion. In his calculations he assumed parallel flow and neglected terms of order δ/R^* (R^* – radius of the wall curvature, Fig.24a). Many attempts were

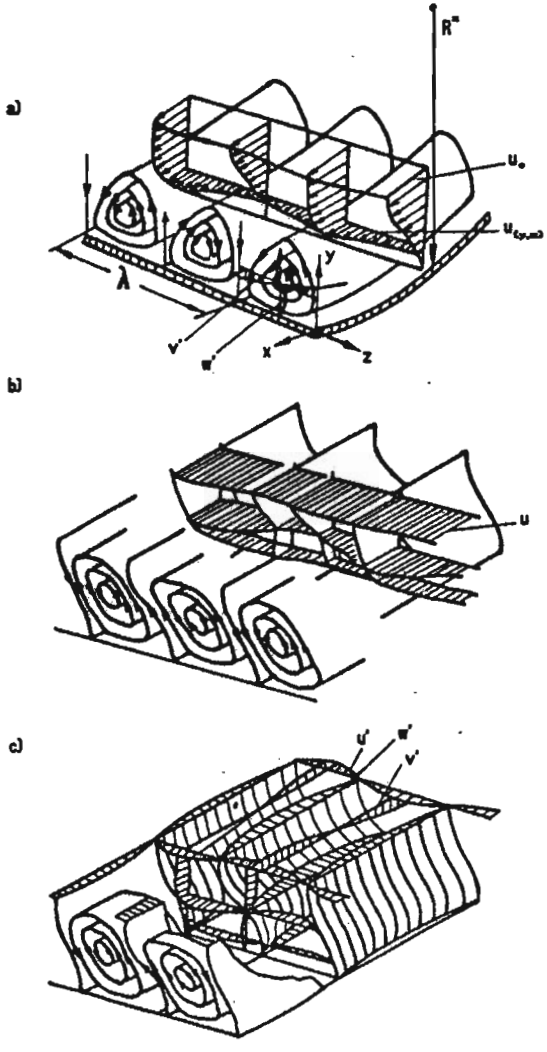

Fig. 24. Development of instability along a concave wall: a) primary instability; b) second-order instability; c) third-order instability, Wortmann (1969)

made to correct and extend the Görtler's analysis. The review of these works, with comparison of resulting neutral curves (Fig.25), can be found in Herbert (1976).

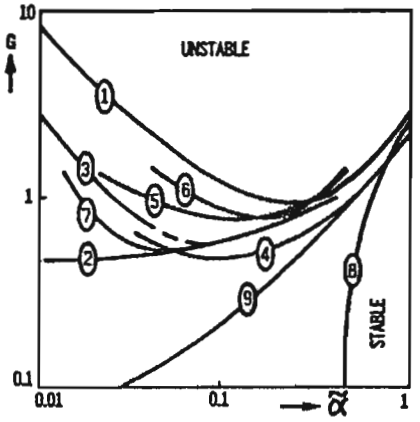

Fig. 25. Neutral curves obtained from different models and different computation procedures of the Görtler instability, Herbert (1976): 1 – Görtler; 2, 3, 5 – Hammerlin; 4 – Smith; 6 – Schultz-Grünow and Behbahani; 7, 8 – Kahawita and Meroney; 9 – Floryan and Saric

In Fig.25 the spanwise wave number $\tilde{\alpha}$ is normalized with the reference length $\delta_r = \sqrt{\nu x_0/U_e}$ (x_0 is the dimensional chordwise location) and G is the Görtler number defined in the following manner

$$G = \sqrt{\mathrm{Re}K} \tag{7.2}$$

The Reynolds number in the above relation is based on reference length δ_r and K is the surface curvature normalized with δ_r.

It is clear that the discrepancies between the various curves are large. The discrepancies between these curves can be attributed to the treatment of the streamvise curvature, treatment of the boundary layer growth and computational accuracy. More recently Floryan and Saric (1979), Ragab and Nayfeh (1979) received better agreement of their results. The linear development of Görtler vortices in growing boundary layer was investigated by Hall (1983). The influence of wall curvature oscillations on Görtler vortices was studied by Jallade (1989) (the asymptotic method).

The concave lower surface in the leading edge region of supersonic airfoil was theoretically analyzed by Collier and Malik (1987). They found that at low sweep the instability is of centrifugal type. For bigger sweep (when the crossflow Reynolds number increases) the crossflow instability will occur. Hall (1985) showed that centrifugal instability is unimportant in the concave region of swept wings if the sweep angle was large in comparison with $\mathrm{Re}^{-1/2}$. This condition is easily satisfied

so in this region of swept wings we can expect the crossflow rather than the Görtler breakdown to turbulence.

8. Waves interactions

A 3D boundary layer is rich in different instability modes such as T–S waves, crossflow vortices, Görtler vortices. A major unanswered question concerning swept wing is about the interaction of these different disturbances.

In the early LFC work Bacon (1962) noticed a somewhat anomalous behavior of transition when sound was introduced in the presence of crossflow vortices. Klebanoff (1962) showed that the onset of 3D structure is quickly followed by the breakdown of the laminar flow and "various instabilities have been found to interact". It is well known that streamwise vortices in the boundary layer strongly influence the behavior of other disturbances.

Nayfeh (1981) analyzed a 2D boundary layer (nonparallel spatial theory) and found that a finite Görtler vortex could interact with two oblique T–S waves of spanwise wavelength twice that of the Görtler. He showed that Görtler vortices produce a double-exponential growth of T–S waves. The concept of double exponential growth was also suggested by Herbert and Morkovin (1980) for the interaction of finite-amplitude of T–S waves with Görtler vortices. Floryan and Saric (1984) showed a similar behavior for streamwise vortices interacting with Görtler vortices.

At the swept wing the most important problem is the crossflow/T–S interaction. If the crossflow vortex structure continues into the midchord region where T–S waves are amplified, the crossflow/T–S interaction could appear and cause premature transition. Reed (1984) showed that the interaction of the crossflow vortices with T–S waves produces a double-exponential growth of T–S waves. Boeing Commercial Airplane Company, in the case when both crossflow and T–S waves occur, proposed the relation (useful for engineering design) between amplification factor for steady crossflow transition N_{CF} and T–S transition N_{TS} (Reed and Saric, 1989)

$$N_{TS} = 12 - 1.2N_{CF} \tag{8.1}$$

In her more recent paper Reed (1988) considered the crossflow/crossflow interaction in the leading edge region of swept wing (disturbance streamlines in the crossflow plane are shown in Fig.26b). Reed explained theoretically, using her interaction theory, the anomalies found in the Saric and Yeates (1985) experiments. In their visualization observations they found vortices at the wavelength predicted by the linear stability theory. However, using hot wire measurements they found that the second harmonic with three times the amplitude of the primary wave was

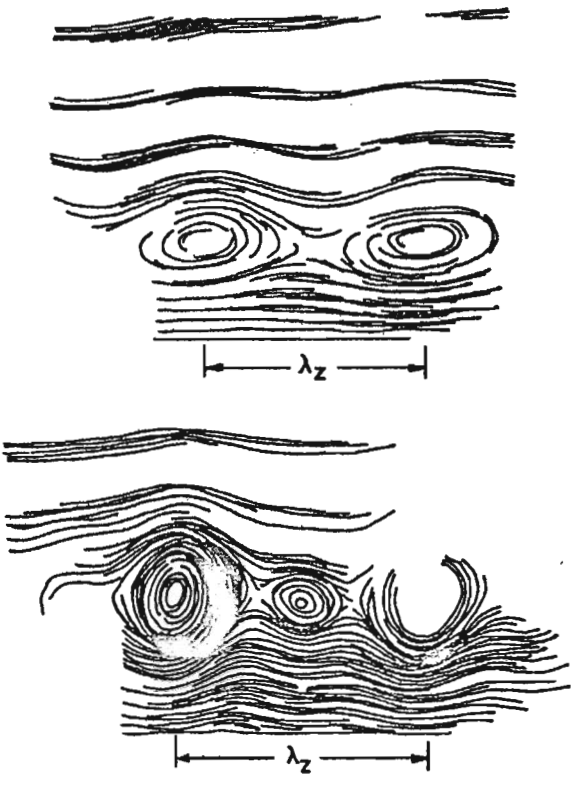

Fig. 26. Calculations of disturbance streamlines in the crossflow plane: a) without interaction; b) in the case of crossflow/crossflow interaction, Reed (1988)

dominant. In such cases the basic transition prediction method based on the linear stability theory would fail. In fact detailed crossflow stability experiments such as Poll (1985), Michel et al. (1985), Saric and Yeates (1985) are few in number. Detailed research is still required because the nature of crossflow vortex structure is still not fully understood.

Wave interactions are also investigated theoretically in Malik (1986), Hall and Smith (1989), Balachander and Streett (1989).

9. Transition prediction – e^N method

Along with efforts to understand the physical processes governing the transition from laminar to turbulent flow, numerous attempts have been undertaken to

predict the point of occurrence of transition. Because our knowledge of transition is not complete, the prediction methods to a great extent have to be based on empirical data.

The state-of-the-art method for predicting transition is the e^N method based on the linear stability theory. It was noted by comparing a large number of experimental data that the transition Reynolds number (based on the freestream speed and the distance from the leading edge) could be satisfactorily correlated with fixed value of N

$$\frac{A}{A_0} = \exp\Big(\int_{x_0}^{x} -\alpha_i dx\Big) = \exp(N) \tag{9.1}$$

It was shown that transition occurs when N approaches 10. That is, the amplitude of the disturbance at transition is e^{10} times larger than the amplitude at the lower branch of neutral stability curve. The e^N method was originally proposed by Smith and Gamberoni (1956), Van Ingen (1956) and recently reviewed by Bushnell et al. (1988). Malik and Orszag (1980) in their paper compared different versions of e^N method and they concluded that the so-called envelope method was the most efficient one.

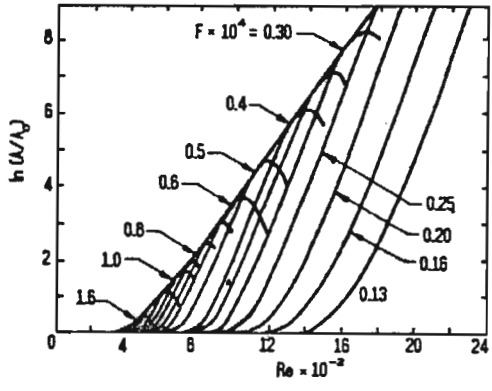

Fig. 27. Blasius boundary layer – $\ln(A/A_0)$ as function of Re for several frequencies, plus envelope curve

For 2D incompressible flows in the envelope procedure, the solution of Orr-Sommerfeld begins at a Reynolds number slightly the greater than critical Reynolds number crRe and frequency from the lower branch of neutral stability curve (Fig.3). As a result of this calculation the wave number α is obtained. Such calculations are made for the subsequent Reynolds numbers (keeping frequency constant). This leads to one of the amplification lines shown in Fig.27. The process is repeated to obtain amplification curves for different values of frequency. As

can be seen from Fig.27 the envelope of the resulting curves corresponds to the maximum amplification factors. From envelope curve the transition point can be obtained by assuming a value of N.

This envelope procedure is useful and convenient for 2D flows. The envelope procedure for the 3D incompressible flow can be found in Srokowski and Orszag (1977) (SALLY code). Srokowski and Orszag calculated maximum temporal amplification rate for given frequency from the incompressible stability equations. They used real part of the group velocity (Eq (3.20)) to convert the temporal amplification rate into spatial one. Then they calculated N by integrating spatial amplification rate along the trajectory defined by the real part of the group velocity.

In, 1982 the computer code COSAL (compressible version of SALLY) was developed by Malik et al. (1982). Work on developing more fundamental methods of stability analysis for swept wing boundary layer were carried out by Cebeci and Stewartson (1980a,b), Nayfeh (1980), Lekoudis (1979) and (1980).

The e^N method is well adapted to design studies. The design of modern laminar-flow-control aircrafts depends on the prediction of the growth of the disturbances in the boundary layer. These designs are carried out with use of advanced computer codes (Campbell, 1987). In the basic LFC technique (suction) the physical parameters are changed so that N would be kept within reasonable limits in order to prevent transition. As long as laminar flow is maintained and the disturbances remain linear, the e^N technique can accurately predict disturbance behavior and can be used to calculate the effectiveness of a particular LFC device. The e^N method is acceptable for design studies as long as different amplified disturbances do not occur simultaneously. At present there is no suitable criterion for establishing transition when both crossflow and T–S waves are present.

As a transition prediction devise, the e^N technique has been the subject of criticism. A major difficulty in the prediction of transition is that transition depends very strongly on environment. Transition is a result of external disturbances which interact with the boundary layer to cause transition either through instability waves or in a more direct manner (bypass). Since in the e^N method no account can be made of the initial disturbances, this method will always be suspected of causing large errors and should be used with the extreme care. The success of e^N correlation is partly due to the fact that the experimental results, on which the method is based, were obtained in wind tunnels where the disturbances of free-stream are similar (particularly the free-stream turbulence level was rather low). In flight conditions the free-stream disturbances can vary in a random manner with no statistical uniformity. When bypasses occurs (high level of the free-stream turbulence) this method does not work at all. The method could be made more realistic by relating the factor N directly to the disturbance level of the source responsible for transition (Mack, 1977). However, transition prediction methods

will remain conditional until the receptivity problem is solved and bypass mechanisms are cleared up. Receptivity problem is still not well understood because of formidable theoretical and experimental difficulties but to achieve real progress in transition prediction a way must be found to deal with the instability waves in terms of the disturbances that cause them.

Appendix 1

The coefficient matrix of compressible stability equations, Mack (1984)

$$a_{12} = 1 \tag{A.1}$$

$$a_{21} = \frac{\mathrm{iRe}}{\mu T}(\alpha U + \beta W - \omega) + \alpha^2 + \beta^2 \tag{A.2}$$

$$a_{22} = -\frac{1}{\mu}\frac{d\mu}{dT}DT \tag{A.3}$$

$$a_{23} = \frac{\mathrm{Re}}{\mu T}(\alpha DU + \beta DW) - \mathrm{i}(\alpha^2 + \beta^2)\frac{1}{\mu}\frac{d\mu}{dT}DT - \\ -\mathrm{i}\frac{1}{3}(1 + 2d)(\alpha^2 + \beta^2)\frac{DT}{T} \tag{A.4}$$

$$a_{24} = \frac{\mathrm{iRe}}{\mu}(\alpha^2 + \beta^2) - \frac{1}{3}(1 + 2d)(\alpha^2 + \beta^2)\gamma \mathrm{Ma}_e^2(\alpha U + \beta W - \omega) \tag{A.5}$$

$$a_{25} = \frac{1}{3}(1 + 2d)(\alpha^2 + \beta^2)\frac{\alpha U + \beta W - \omega}{T} - \frac{1}{\mu}\frac{d\mu}{dT}(\alpha D^2 U + \beta D^2 W) - \\ -\frac{1}{\mu}\frac{d^2\mu}{dT^2}DT(\alpha DU + \beta DW) \tag{A.6}$$

$$a_{26} = -\frac{1}{\mu}\frac{d\mu}{dT}(\alpha DU + \beta DW) \tag{A.7}$$

$$a_{31} = -\mathrm{i} \tag{A.8}$$

$$a_{33} = \frac{DT}{T} \tag{A.9}$$

$$a_{34} = -\mathrm{i}\gamma \mathrm{Ma}_e^2(\alpha U + \beta W - \omega) \tag{A.10}$$

$$a_{35} = \frac{\mathrm{i}}{T}(\alpha U + \beta W - \omega) \tag{A.11}$$

$$a_{41} = -\frac{\mathrm{i}}{E}\left[\frac{2}{\mu}\frac{d\mu}{dT}DT + \frac{2}{3}(2 + d)\frac{DT}{T}\right] \tag{A.12}$$

$$a_{42} = -\frac{\mathrm{i}}{E} \tag{A.13}$$

$$a_{43} = \frac{1}{E}\left[-(\alpha^2 + \beta^2) + \frac{2}{3}(2 + d)\frac{DT^2}{T}\frac{1}{\mu}\frac{d\mu}{dT} + \frac{2}{3}(2 + d)\frac{D^2T}{T} -\right.$$

$$-\frac{\mathrm{iRe}}{\mu T}(\alpha U+\beta W-\omega)\Big] \tag{A.14}$$

$$a_{44}=-\frac{\mathrm{i}}{E}\frac{2}{3}(2+d)\gamma \mathrm{Ma}_e^2\Big[(\alpha U+\beta W-\omega)\frac{1}{\mu}\frac{d\mu}{dT}DT+$$

$$+\alpha DU+\beta DW+\frac{DT}{T}(\alpha U+\beta W-\omega)\Big] \tag{A.15}$$

$$a_{45}=\frac{\mathrm{i}}{E}\Big\{\frac{1}{\mu}\frac{d\mu}{dT}(\alpha DU+\beta DW)+\frac{2}{3}(2+d)\cdot$$

$$\cdot\Big[\frac{1}{\mu}\frac{d\mu}{dT}\frac{DT}{T}(\alpha U+\beta W-\omega)+\frac{\alpha DU+\beta DW}{T}\Big]\Big\} \tag{A.16}$$

$$a_{46}=\frac{\mathrm{i}}{E}\frac{2}{3}(2+d)(\alpha U+\beta W-\omega) \tag{A.17}$$

$$a_{56}=1 \tag{A.18}$$

$$a_{62}=-2\sigma(\gamma-1)\mathrm{Ma}_e^2\frac{\alpha DU+\beta DW}{\alpha^2+\beta^2} \tag{A.19}$$

$$a_{63}=\frac{\mathrm{Re}\sigma}{\mu}\frac{DT}{T}-\mathrm{i}2\sigma(\gamma-1)\mathrm{Ma}_e^2(\alpha DU+\beta DW) \tag{A.20}$$

$$a_{64}=-\mathrm{i}\frac{\mathrm{Re}\sigma}{\mu}(\gamma-1)\mathrm{Ma}_e^2(\alpha U+\beta W-\omega) \tag{A.21}$$

$$a_{65}=\mathrm{i}\frac{\mathrm{Re}\sigma}{\mu T}(\alpha U+\beta W-\omega)+\alpha^2+\beta^2-\frac{D^2T}{\kappa}\frac{d\kappa}{dT}-\frac{DT^2}{\kappa}\frac{d^2\kappa}{dT^2}-$$

$$-\sigma(\gamma-1)\mathrm{Ma}_e^2\frac{1}{\mu}\frac{d\mu}{dT}(DU^2+DW^2) \tag{A.22}$$

$$a_{66}=-\frac{2}{\kappa}\frac{d\kappa}{dT}DT \tag{A.23}$$

$$a_{68}=-2\sigma(\gamma-1)\mathrm{Ma}_e^2\frac{\alpha DW-\beta DU}{\alpha^2+\beta^2} \tag{A.24}$$

$$a_{78}=1 \tag{A.25}$$

$$a_{83}=\frac{\mathrm{Re}}{\mu T}(\alpha DW-\beta DU) \tag{A.26}$$

$$a_{85}=-\frac{1}{\mu}\frac{d\mu}{dT}(\alpha D^2W-\beta D^2U)-\frac{1}{\mu}\frac{d^2\mu}{dT^2}DT(\alpha DW-\beta DU) \tag{A.27}$$

$$a_{86}=-\frac{1}{\mu}\frac{d\mu}{dT}(\alpha DW-\beta DU) \tag{A.28}$$

$$a_{87}=\frac{\mathrm{iRe}}{\mu T}(\alpha U+\beta W-\omega)+\alpha^2+\beta^2 \tag{A.29}$$

$$a_{88}=-\frac{1}{\mu}\frac{d\mu}{dT}DT \tag{A.30}$$

$$E=\frac{\mathrm{Re}}{\mu}+\mathrm{i}\frac{2}{3}(2+d)\gamma\mathrm{Ma}_e^2(\alpha U+\beta W-\omega) \tag{A.31}$$

In these equations, the ratio of the second to the first viscosity coefficient

$$d = \frac{\lambda}{\mu} \tag{A.32}$$

is taken by Mack (1984) to be constant and equal to 1.2 (Stokes' assumption corresponds to $\lambda = 0$). In the numerical computations Mack used

$$\mu^* 10^5 = \begin{cases} 1.458 \dfrac{\sqrt{T^{*3}}}{T^* + 110.4} & T^* > 110.4K \\ 0.0693873 T^* & T^* < 110.4K \end{cases} \tag{A.33}$$

for the viscosity coefficient in cgs units, and

$$\kappa^* = 0.6325\sqrt{T^*}\left[1 + \frac{245.4}{T^*} 10^{\frac{-12}{T^*}}\right]^{-1} \tag{A.34}$$

for the thermal conductivity coefficient in cgs units. The Prandtl number is defined

$$\sigma = \frac{c_p \mu^*}{\kappa^*} \tag{A.35}$$

where c_p is a specific heat.

Acknowledgment

The author is most grateful to Prof. Dipl.-Ing. Walter Riess from the University of Hannover for the extensive help to her during the scholarship .

References

1. ARNAL D., 1984, *Description and prediction of transition in two-dimensional incompressible flow,* AGARD Report 709
2. BACON J., PFENNINGER W., MOORE C., 1962, *Influence of acustical disturbances on the behaviour of a swept laminar suction wing,* Northrop Rep. NOR-62-124
3. BALACHANDER S., STREETT C., 1989, *Numerical simulation of transition in a rotating disk flow,* Instability and Transition, II, Springer Verlag
4. BENNEY D.J., LIN C.C., 1960, *On the secondary motion induced by oscillations in a shear flow,* Phys.Fluids, 3
5. BRASLOW A., FISCHER M., 1985, *Design considerations for application of laminar flow control systems for transport aircraft,* AGARD Report 723
6. BROWN F., 1959, *The organized boundary layer,* Proceedings of the Sixth Midwestern Conference on Fluid Mechanics (University of Texas, Austin, Texas)

7. BUSHNELL D.M., MALIK M.R., HORVEY W.D., 1988, *Transition prediction in external flow via linear stability theory,* IUTAM Symposium Transonicum III, Göttingen

8. CAMPBELL R.L., 1987, *A hybrid algorithm for transonic airfoil and wing design,* AIAA Pap., 87-2552

9. CEBECI T., STEWARTSON K., 1980A, *On stability and transition in three-dimensional flows,* AIAA J., **18**, 4, 398-405

10. CEBECI T., STEWARTSON K., 1980B, *On the prediction of transition in three-dimensional flows,* Laminar Turbulent Transition, (R.Eppler and H.Fasel), Springer Verlag, Berlin

11. COLLIER F.S.JR., MALIK M.R., 1987, *Stationary disturbances in three-dimensional boundary layers over concave surfaces,* AIAA Pap., 87-1412

12. CRAIK A.D.D., 1971, *Non-linear resonant instability in boundary layers,* J.Fluid Mech., **50**, Part 2

13. FASEL H.F., RIST U., KONZELMANN U., 1987,*Numerical investigation of the three-dimensional development in boundary layer transition,* AIAA Pap., 87-1203

14. FLORYAN J., SARIC. W., 1979, *Stability of Görtler vortices in boundary layers,* AIAA J., **20**, 3, 316-24

15. FLORYAN J.M., SARIC W., 1984, *Wave-length selection and growth of Görtler vortices,* AIAA J., 22, 1529-38

16. GASTER M., 1967, *On the flow along swept leading edges,* Aeronaut.Q., **18**, 5, 165-84

17. GASTER M., 1975, *A theoretical model of a wave packet in the boundary layer on a flat plate,* Proc.R.Soc.London, Ser. A 347, 271-89

18. GÖRTLER H., 1954, *On the three-dimensional instability of laminar boundary layers on concave walls,* NACA Tech. Memo., 1375

19. GRAY W.E., 1952, *The effect of wing sweep on laminar flow,* RAE TM Aero., 255

20. GREGORY N., STUART J., WALKER W., 1955, *On stability of three dimensional boundary layers with applications to the flow due to a rotating disk,* Philos,Trans.R.Soc.London, Ser. A 248, 155-99

21. HALL P., 1983, *The linear development of Görtler vortices in growing boundary layers,* J.Fluid Mech., **130**, 41-58

22. HALL P., 1985, *The Görtler vortex instability mechanism in the three-dimensional boundary layers,* Proc.R.Soc.London, Ser. A 399, 135-52

23. HALL P., MALIK M.R., 1986, *On the instability of a three-dimensional attachment-line boundary layer: weakly nonlinear theory and a numerical approach,* J.Fluid Mech., 163, 257-82

24. HALL P., MALIK M. R., POLL, D., 1984, *On the stability of an infinite swept attachment-line boundary layer,* Proc.R.Soc.London, Ser.A 395, 229-45

25. HALL P., SMITH F.T., 1989, *Non-planar T-S waves and longitudinal vortices in channel flow: nonlinear interaction and focussing,* Instability and Transition, II, Springer Verlag

26. HERBERT T., 1976, *On the stability of the boundary layer along a concave wall,* Archiwum Mechaniki Stosowanej, **28**, 5-6, 1039-55

27. HERBERT T., 1980, *Nonlinear stability of parallel flows by high-order amplitude expansions,* AIAA J., **18**, 3

28. HERBERT T., 1983A, *On perturbation methods in nonlinear stability theory,* J.Fluid Mech., **126**, 167-86

29. HERBERT T., 1983B, *Subharmonic three-dimensional disturbances in unstable plane shear flows,* AIAA Pap., 83-1759

30. HERBERT T., 1984A, *Nonlinear effects in hydrodynamic stability,* AGARD Report 709

31. HERBERT T., 1984B, *Secondary instability of shear flows,* AGARD Report 709

32. HERBERT T., 1988, *Secoundary instability of boundary layers,* Ann.Rev.Fluid Mech., 20, 487-526

33. HERBERT T., MORKOVIN M.V., 1980, *Dialogue on bridging some gaps in stability and transition research,* In Laminar Turbulent Transition, ed. R.Eppler.H.Fasel, 47-72, Berlin, Springer Verlag

34. HUSSAINI M.Y., ZANG T., 1987, *Spectral methods in fluid dynamics,* Ann. Rev.Fluid Mech., 19, 339-68

35. JALLADE S., 1989, *Effects of streamwise curvature variations on Görtler vortices,* Instability and Transition, II, Springer Verlag

36. KACHANOV YU.S., LEVCHENKO V., 1984, *Resonant interactions of disturbances in transition to turbulence in a boundary layer,* J.Fluid Mech., **138**

37. KARMAN TH. VON, 1921, *Laminare und turbulente Reibung,* ZAMM, **1**, 233-52

38. KLEBANOFF P., TIDSTROM K., SARGENT L., 1962, *The three-dimensional nature of boundary layer instability,* J.Fluid Mech., **12**, 1-34

39. KNAPP C., ROACHE P., MUELLER T., 1968, *A combined visual and hot-wire anemometer investigation of boundary layer transition,* AIAA J., 6, 29-36

40. KOBAYASHI R., 1981, *Linear stability theory of boundary layer along a cone rotating in axial flow,* Bull.Jpn.Soc.Mech.Eng., 24, 934-40

41. KOBAYASHI R., KOHAMA Y., 1984, *Spiral vortices in boundary layer transition on a rotating cone,* Laminar Turbulent Transition; IUTAM Symposium, Novosibirsk, 573-80

42. KOBAYASHI R., IZUMI H., 1983, *Boundary layer transition on a rotating cone in still fluid* , J.Fluid Mech., **127**, 353-364

43. KOBAYASHI R., KOHAMA Y., ARAI T., UKAKU M., 1987, *The boundary layer transition on rotating cones in axial flow with free-stream turbulence,* JSME Int.J, 30(261)

44. KOBYASHI R., KOHAMA Y., KUROSAWA M., 1983, *Boundary layer transition on a rotating cone in axial flow,* J.Fluid Mech., **127**, 341-52

45. KOBAYASHI R., KOHAMA Y., TAKAMADATE CH., 1980, *Spiral vortices in boundary layer transition regime on a rotating disk,* Acta Mechanica, 35, 71-82

46. KOHAMA Y., 1984, *Behavior of spiral vortices on a rotating cone in axial flow,* Acta Mechanica, **51**, 105-117

47. KOHAMA Y., 1984, *Study on boundary layer transition of a rotating disk,* Acta Mechanika, 50, 193-99

48. KOHAMA Y., 1985, *Turbulent transition process of the spiral vortices appearing in the laminar boundary layer of a rotating cone,* Phys.Chem.Hydrodyn., 6(5)

49. KOHAMA Y., 1986, *Coherent structure in three dimensional boundary layer transition,* Proc.Asian.Congr.Fluid Mech. 3rd, Tokyo

50. KOHAMA Y., 1987A, *Crossflow instability in rotating disk boundary layer,* AIAA Pap., 87-1340

51. KOHAMA Y., 1987B, *Some expectation on mechanism of crossflow instability on a swept wing flow,* Acta Mechanica 66, 21-38

52. KOHAMA Y., 1987C, *Some similarities in the breakdown process of the primary instability between 2-D and 3-D boundary layer,* Phys.Chem.Hydrodyn., 9, 1/2, 209-18

53. KOHAMA Y., KOBAYASHI R., 1983A, *Behaviour of spiral vortices on rotating axisymetric bodies,* Rep.Inst.High Speed Mech., Tohoku University, Japan, 43, 365

54. KOHAMA Y., KOBAYASHI R., 1983B, *Boundary layer transition and the behaviour of spiral vortices on rotating sphere,* J.Fluid Mech., 137, 153-164

55. KOZLOV V.V., LEVCHENKO V., SARIC W., 1984, *Formulation of three-dimensional structures on the transition to turbulence in boundary layer,* Izvestiya Akademii Nauk SSSR, Mekhanika Zhidkosti i Gaza, 6, 42-50

56. KOZLOV V.V., RAMAZONOV M.P., 1984, *Development of finite amplitude disturbances in Poiseulle flow,* J.Fluid Mech., 147

57. LEES L., LIN C., 1946, *Investigation of the stability of the laminar boundary layer in compressible fluid,* NACA TN-1115

58. LEES L., ROSHOTKO E., 1962, *Stability of the compressible laminar boundary layer,* J.Fluid Mech., 12, 555-90

59. LEKOUDIS S., 1979, *Stability of three-dimensional compressible boundary layers over wings with suction,* AIAA Paper 79-1495

60. LEKOUDIS S., 1980, *Stability of the boundary layer on a swept wing with wall cooling,* AIAA J., 18, 1029-35

61. LIEPMANN H.W., 1982, *Active control of laminar-turbulent transition,* J. Fluid Mech., 118

62. MACK, L.M., 1977, *Transition prediction and linear stability theory,* AGARD CP, 224

63. MACK L.M., 1979, *On the stability of the boundary layer on a transonic swept wing,* AIAA Pap., 79-0264

64. MACK L.M., 1984, *Boundary layer linear stability theory,* AGARD Report 709

65. MACK L.M., 1985, *The wave pattern produced by point source on a rotating disk,* AIAA Pap., 85-0490

66. MALIK M.R., 1986, *Wave interactions in the three-dimensional boundary layers,* AIAAA Pap., 86-1129

67. MALIK M.R., CHUANG S., HUSSAINI M., 1982, *Accurate numerical solution of compressible linear stability equations,* ZAMP 33, 189-201

68. MALIK M.R., ORSZAG S.A., 1980, *Comparison of methods for prediction of transition by stability analysis,* AIAA J., 18, 12

69. MALIK M.R., POLL D., 1984, *Effect of curvature on three dimensional boundary layer stability,* AIAA Pap., 84-1672

70. MALIK M.R., WILKINSON S.P., ORSZAG S.A., 1981, *Instability and transition in rotating disk flow,* AIAA J., 19(9), 1131-38

71. MICHEL R., ARNAL D., COUSTOLS E., JUILLEN J., 1985, *Experimental and theoretical studies of boundary layer transition on a swept infinite wing*, Laminar Turbulent Transition, New York, Springer Verlag, 553-61

72. MORKOVIN M.R., 1978, *Instability, transition to turbulence and predictability*, AGARDograph, 236

73. NAYFEH A., 1980, *Stability of three dimensional boundary layer*, AIAA J., **18**, 4, 406-16

74. NAYFEH A. H., 1981, *Effect of streamwise vortices on Tollmien-Schlichting waves*, J. Fluid Mech., **107**, 441-53

75. ORSZAG S. A., KELLS L., 1980, *Transition to turbulence in plane Poiseuille and plane Couette flow*, J.Fluid Mech. 96, 159-205

76. OWEN P.R., RANDALL D.J., 1952, *Boundary layer transition on the swept wing*, RAE TM Aero., 277

77. PADHYE A., NAYFEH A., 1981, *Nonparallel stability of three dimensional flows*, AIAA Pap., 81-1281

78. POLL D., 1977, *Leading edge transition on swept wings*, AGARD CP 224

79. POLL D., 1979, *Transition in he infinite swept attachment line boundary layer*, Aero.Q., 30, 607-29

80. POLL D., 1981, *Skin friction and heat transfer at an infinite swept attachment line*, Aeronaut.Q., 32, 299-318

81. POLL D., 1984, *Transition description and prediction in three-dimensional flows*, AGARD Report, 709

82. POLL D., 1985, *Some observations of the transition process on the windward face of a long yawed cylinder*, J.Fluid Mech., 150, 329-56

83. PRANDTL L., 1921, *Bemerkunger uber die Enstehung der Turbulenz*, ZAMM, **1**, 431-36

84. RAGAB S.A., NAYFEH A.H., 1979, *On Görtler instability*, Virginia Politechnic Institute and State University, Blacksburg, VA 24061

85. RAYLEIGH, LORD, 1887, *On the stability or instability of certain fluid motions*, Scientific Papers, Cambridge Univ.Press., Cambridge, **3**, 17-23

86. REED H., 1984, *Wave interactions in swept wing flows*, AIAA Pap., 84-1678

87. REED H., 1988, *Wave interaction in swept wing flows*, Phys.Fluids, 30(11), 3419-26

88. REED H., SARIC W., 1989, *Stability of three dimensional boundary layers*, Ann.Rev.Fluid Mech., 21, 235-84

89. ROSHOTKO E., 1984, *Environment and receptivity*, AGARD Report 709

90. SARIC W., 1985A, *Boundary layer transition: T-S waves and crossflow mechanism*, AGARD Report, 723

91. SARIC W., 1985B, *Laminar flow control with suction: theory and experiment*, AGARD Report, 723

92. SARIC W., 1986, *Boundary layer transition to turbulence: the last five years*, Tenth Symposium on Turbulence

93. SARIC W., YEATES L., 1985, *Experiments on the stability of crossflow vortices in swept wing flows*, AIAA 23rd Aerospace Sciences Meeting, Nevada

94. SCHLICHTING H., 1933, *Zur Entstehung der Turbulenz bei der Plattenströmung*, Nachr.Gas.Wiss., Göttingen, Math.-Phys.Klasse, 191-208

95. SCHUBAUER G.B., SKRAMSTAD H.K., 1947, *Laminar boundary layer oscillations and transitions on a flat plate*, J.Aero.Sci., 14, 69-76

96. SINGER B.A., MAYER F., KLEISER L., 1989, *Nonlinear development of crossflow vortices*, Instability and Transition, II, Springer-Verlag

97. SINGER B.A., REED H.L., FERZIGER J.H., 1986, *Investigation of the effects of initial disturbances on plane channel transition*, AIAA Pap., 86-0433

98. SMITH A.M., GAMBERONI N., 1956, *Transition, pressure gradient and stability theory*, Dauglas Aircr.Co., Inc., ES 26388

99. SPALART P., YANG K., 1987, *Numerical study of ribbon-induced transition in Blasius flow*, J.Fluid Mech., 178, 345-65

100. SROKOWSKI A., ORSZAG S.A., 1977, *Mass flow requirement to LFC wing design*, AIAA Pap., 77-1222

101. THOMAS A., 1985, *Aircraft drag reduction technology – a summary*, AGARD Report No.723

102. TOLLMIEN W., 1935, *Ein allgemeines Kriterium der Instabiltät Laminarer Geschwindigkeitsverteilungen*, Nachr. Gas. Wiss., Göttingen, Math.-Phys.Klasse, 50, 79-114

103. VAN INGEN J., 1956, *A suggested semi-empirical method for the calculation of the boundary layer transition region*, Rep. VTH 71 and 74, Dep.Aeronaut.Eng., Univ.Technol.Delft Holland, 1956

104. WORTMANN F., 1969, *Visualization of transition*, J.Fluid Mech., 38, 3

Niestabilność trójwymiarowej warstwy przyściennej

Streszczenie

Konstrukcje nowoczesnych samolotów o kontrolowanej warstwie przyściennej zależą od poznania zjawisk prowadzących do powstania turbulentnej warstwy przyściennej. Jednak pomimo ogromnego wysilku badawczego zarówno źródla turbulencji jak i sam proces przejścia laminarno-turbulentnego pozostają ciągle jednymi z najważniejszych nierozwiązanych problemów aerodynamiki. W artykule przedstawiono przegląd prac eksperymentalnych i teoretycznych dotyczących niestabilności trójwymiarowej warstwy przyściennej. Analizowane są cztery rodzaje niestabilności: skażenie krawędzi natarcia, niestabilność lepka, niestabilność crossflow oraz niestabilność odśrodkowa. Omawiana jest metoda e^N przewidywania punktu wystąpienia przejścia laminarno-turbulentnego.

Manuscript received April 30, 1992; accepted for print September 29, 1992